

## COMMUNICATION

## A tolane-modified 5-ethynyluridine as universal and fluorogenic photochemical DNA crosslinker

Hermann Neitz<sup>a</sup> and Claudia Höbartner<sup>\*a,b</sup>

Received 00th January 20xx,  
Accepted 00th January 20xx

DOI: 10.1039/x0xx00000x

**We report the fluorescent nucleoside <sup>Tol</sup>dU and its application as photoresponsive crosslinker in three different DNA architectures with enhanced fluorescence emission of the crosslinked products. The fluorogenic <sup>Tol</sup>dU crosslinking enables the assembly of DNA polymers in a hybridisation chain reaction for the concentration-dependent detection of a specific DNA sequence.**

Fluorescent nucleobase analogues are of great interest in nucleic acid chemistry.<sup>1</sup> The lack of fluorescence in natural nucleosides provides the opportunity for developing novel reporters,<sup>2</sup> which are sensitive to the local environment, and are useful as biochemical tools for structural characterization,<sup>3</sup> detection of single nucleotide polymorphisms (SNPs)<sup>4</sup> or enzyme activities<sup>5</sup>. The attachment of fluorogenic dyes to natural nucleosides offers the advantage of a precise placement of the chromophore in the DNA/RNA helix,<sup>6</sup> which is also a requirement for proximity induced reactions.<sup>7</sup> The DNA double helix is an outstanding template for organizing reactive groups in suitable arrangements for the formation of a covalent bond between two strands, either in the form of interstrand crosslinking or by sealing a nick in the templated ligation of two single strands hybridized to a matched complementary strand.<sup>8</sup> Of particular interest are photo-controlled crosslinking and ligation reactions, which do not require any additional reagents and enable precise control of product formation.<sup>9</sup> Several examples have been reported for photocontrolled ligation<sup>10</sup> and interstrand crosslinking (ICL) reactions.<sup>11</sup> However, such reactions rarely lead to increased fluorescence.<sup>12</sup> A fluorescence-enhancing templated reaction was recently reported that enabled the multiple-turnover transformation of profluorophores for the detection of DNA sequences.<sup>13</sup> In this work, we report a fluorogenic photoinduced DNA ligation reaction that is compatible with concentration-dependent signal amplification in a hybridization chain reaction using 5-[4-

(phenylethynyl)phenylethynyl]-2'-deoxyuridine (<sup>Tol</sup>dU) as a novel fluorescent nucleoside analogue. When incorporated into three different DNA architectures, we found that two adequately arranged <sup>Tol</sup>dU units undergo an efficient light-induced intermolecular crosslinking reaction that results in enhanced fluorescence emission (Fig 1).

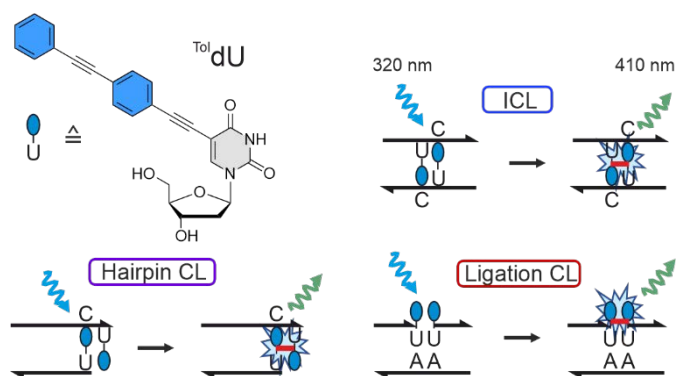


**Fig. 1.** Structure of <sup>Tol</sup>dU nucleoside and three DNA architectures for <sup>Tol</sup>dU crosslinking investigated in this work: internal interstrand crosslink (ICL), terminal interstrand crosslink for hairpin formation, and linear ligation crosslink.

Phenylene ethynylene units have been introduced as rigid hydrophobic moieties into oligonucleotides for the synthesis of DNA amphiphiles<sup>14</sup> and as energy-transfer spacers for the attachment of fluorophores in the major groove of DNA.<sup>15</sup> Here we investigated <sup>Tol</sup>dU as new fluorescent nucleoside, which formally has a tolane unit linearly attached to 5-ethynyluridine. The <sup>Tol</sup>dU building blocks for solid-phase synthesis were prepared via Sonogashira crosscoupling of 1-ethynyl-4-(2-phenylethynyl)benzene with 5'-O-DMT protected 5-iodo-2'-deoxyuridine (Scheme S1), and converted to the 3'-cyanoethyl diisopropyl phosphoramidite or attached as succinyl ester to long-chain alkyl amino controlled pore glass solid support. The free <sup>Tol</sup>dU nucleoside was obtained by removal of the DMT group and showed an absorption maximum at 328 nm and a fluorescence emission maximum at 397 nm with a quantum yield of 38% in DMSO (Fig S1-S2).

The <sup>Tol</sup>dU moiety was incorporated into DNA strands using standard DNA phosphoramidite chemistry. The DNA sequences

<sup>a</sup> Institute of Organic Chemistry, University of Würzburg, Am Hubland, 97074 Würzburg, Germany.

<sup>b</sup> Center for Nanosystems Chemistry (CNC), University of Würzburg, Theodor-Boveri-Weg, 97074 Würzburg, Germany

\* Footnotes relating to the title and/or authors should appear here.

Electronic Supplementary Information (ESI) available: [details of any supplementary information available should be included here]. See DOI: 10.1039/x0xx00000x

and HR-ESI MS data are given in Table S1. The presence of the <sup>Tol</sup>dU unit was also confirmed by the additional absorption peak around 330 nm in the UV spectra of single strands and <sup>Tol</sup>dU containing duplexes (Fig S3). Thermal melting curves were monitored at 260 nm and revealed a melting temperature of 37.2 °C for the fully complementary duplex, i.e. with adenosine opposite to <sup>Tol</sup>dU (Fig S4, Table S2). This is a slight destabilization of 2.8 °C compared to the analogous duplex with an unmodified dA/dT base pair, but circa 10 °C more stable than the duplexes with mismatched nucleobases or a non-nucleosidic alkyl linker facing <sup>Tol</sup>dU (Fig S4A). The fluorescence of <sup>Tol</sup>dU was examined in matched and mismatched duplexes. The highest fluorescence intensity was observed when <sup>Tol</sup>dU was paired with adenosine (Fig S4B), suggesting a rigid orientation in the base-pair, while the mismatched cases resulted in more flexible orientations reflected in a lower emission intensity. The same trend was confirmed by relative quantum yields and fluorescence lifetimes (Fig S5-S6 and Table S3-S4).

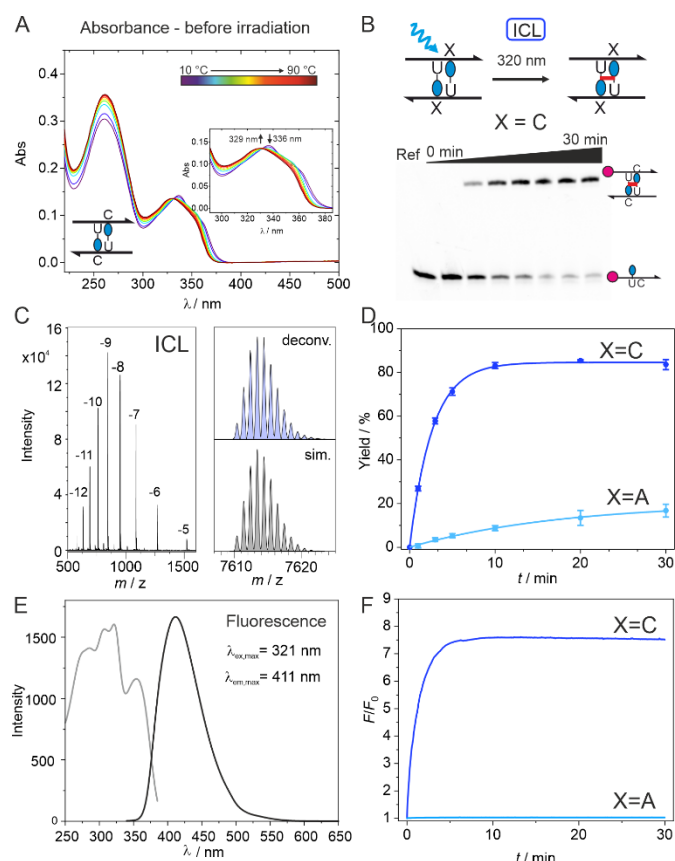


**Fig. 2.** (A) Temperature-dependent UV/Vis spectra of double-modified <sup>Tol</sup>dU/dC duplex reveal hydrophobic stacking interactions at low temperatures in the folded duplex. (B) Schematic representations of the duplex for ICL formation and denaturing PAGE analysis of aliquots removed at specific time intervals. The magenta sphere represents the Cy3 label. (C) ESI-MS of isolated ICL product (left), deconvoluted and simulated mass spectra (right). Calculated monoisotopic mass: 7610.3804 Da, found 7610.3826 Da (error -0.3 ppm). (D) Kinetics of ICL formation via PAGE analysis (see gel image in B). (E) Fluorescence excitation and emission spectra of isolated ICL product (i.e., ICL-containing DNA duplex without Cy3 label). (F) Kinetics of fluorescence increase at 410 nm upon irradiation reports the formation of fluorescent ICL when X=C, but not when X=A. Conditions for kinetics in B, D, F: 1 μM DNA in 10 mM sodium phosphate, 100 mM NaCl, pH 7.0.

The observed mismatch sensitivity of <sup>Tol</sup>dU suggested that hydrophobic stacking interactions between tolane units could be favored when two <sup>Tol</sup>dU nucleosides are incorporated in neighbouring mismatched base pairs. Indeed, stacking interactions were observed by temperature-dependent UV/Vis spectroscopy, in analogy to earlier reports with diphenylacetylene<sup>16</sup> or 4,4'-substituted tolanes<sup>17</sup> incorporated into the DNA backbone. For interacting <sup>Tol</sup>dU units in our DNA duplexes, the absorption maximum shifted slightly to shorter wavelengths (from 336 nm to 329 nm) upon denaturation of the interaction at higher temperatures (Fig 2A), while no temperature-dependent change was observed when both <sup>Tol</sup>dU units were base-paired to adenosine (Fig S7A).

Upon irradiation of the duplexes containing two hydrophobic <sup>Tol</sup>dU nucleosides in pyrimidine mismatches, we observed efficient crosslink formation. With one of the <sup>Tol</sup>dU DNA strands containing a Cy3 label for visualization on denaturing PAGE, more than 80% conversion to the slower-migrating crosslinked product occurred after 10 min of irradiation at 320 nm (Fig 2B, D and S8). The reaction was scaled up, and the crosslinked product was isolated by PAGE. ESI-MS confirmed the formation of the crosslinked product consisting of the two single strands without addition of any other compound (Fig 2C, Fig S9). This observation is consistent with our recent findings with 5-phenylethynyl-uridine (<sup>Phe</sup>dU) nucleosides, for which we found that a stacked dimer in a pyrimidine mismatched orientation easily forms an interstrand crosslink via an alkene-alkyne [2+2] photocycloaddition.<sup>18</sup>

Interestingly, the new <sup>Tol</sup>dU ICL product showed an emission maximum at 411 nm with a quantum yield of 3.9% in the duplex (Fig 2E, Fig S10). The time-dependent increase at the emission wavelength of 410 nm (Fig 2F) showed similar kinetics to the PAGE analysis, and the final fluorescence intensity was up to seven times higher than before crosslinking. We interpret this increase in fluorescence as a result of the enhanced rigidity in the crosslinked product, thus reducing the degree of freedom for thermal non-radiative deactivation of the excited state. To prove the necessity of the mismatched dC/<sup>Tol</sup>dU motif, we examined a duplex sample containing dA/<sup>Tol</sup>dU base pairs instead of the mismatch. The base-paired situation keeps the tolane units oriented towards the major groove of the helix, thus preventing inter-tolane stacking interactions. Indeed, the crosslinking yield was strongly reduced (only low conversion < 20% after 30 min), and no significant fluorescence increase was observed for the fully base-paired <sup>Tol</sup>dU duplex (Fig 2D, F, X=A). To further analyse the ICL product, the crosslinked duplex was enzymatically digested, and the nucleoside mixture was analysed by LC-MS after extraction of the hydrophobic nucleoside dimer into the organic phase (Fig S11, S12). Both MALDI and ESI-MS confirmed the formation of the product containing two <sup>Tol</sup>dU units.

Encouraged by the efficient ICL formation with <sup>Tol</sup>dU in the middle of the duplex, we explored the generality of the approach, and moved the <sup>Tol</sup>dU units to the end of the duplex. Photoinduced crosslinking would then result in the formation of an artificial DNA hairpin that is capped by a covalent <sup>Tol</sup>dU dimer. We synthesized one DNA strand on <sup>Tol</sup>dU-CPG, i.e.

placing the modification at the 3' end. In a complementary DNA oligonucleotide, we incorporated the  $T^{ol}dU$  nucleoside at the 5' end. The two strands were hybridized and crosslink formation upon irradiation at 320 nm was analysed by PAGE and fluorescence spectroscopy (Fig 3, S8). Full conversion to a slower migrating product was observed within 10 min, showing again an eight times higher fluorescence emission at 410 nm. The crosslinked product was isolated and characterized by ESI-MS (Fig S9), revealing the expected mass of the DNA hairpin as the sum of the two  $T^{ol}dU$  containing single strands. The thermal melting curve of the crosslinked  $T^{ol}dU$  hairpin showed an impressive stabilization by 25°C (Fig 3B), comparable to artificial aromatic hairpin caps, such as for example a perylenebisimide covalently connected to the DNA phosphodiester backbone.<sup>19</sup> In a third DNA architecture for  $T^{ol}dU$  crosslinking, we placed the  $T^{ol}dU$  nucleosides at the 5' and 3' ends of a 12 and a 13-mer oligonucleotide, respectively. The two strands were hybridized to a fully complementary 25-nt long DNA template (Fig 3C). In this setup, the tolane units were arranged directly next to each other, both facing the major groove of the nicked duplex. Upon irradiation at 320 nm, a linear ligation product was formed by sealing the nicked 25-mer duplex. This is also confirmed by ESI-MS of the isolated ligation product (Fig S9), and by a single melting transition at 59.6°C of the DNA duplex after irradiation, i.e. containing the ligated product (Fig S14). Again, the crosslinking reaction could also be monitored by fluorescence spectroscopy, and no ligation reaction was observed in the absence of the template (Fig 3D, Fig S15). A structural model of the  $T^{ol}dU$  units in a nicked double helix suggests a possible orientation for formation of a parallel  $T^{ol}dU$  dimer by alkene alkyne photocycloaddition (Fig S13).

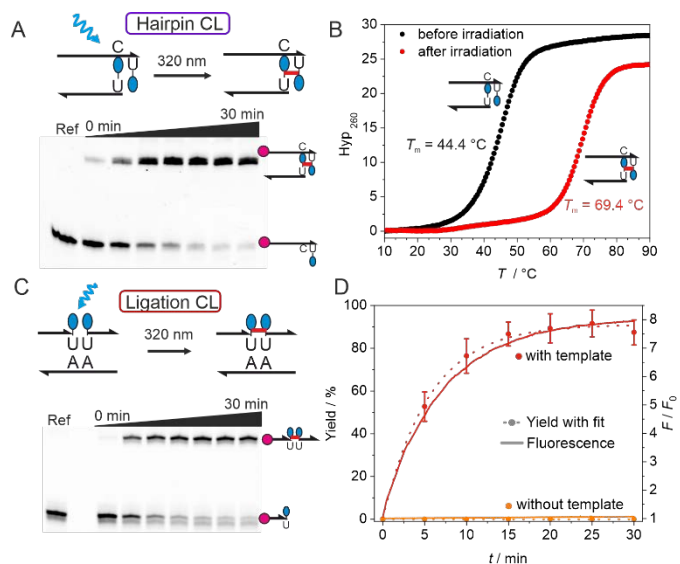


**Fig. 3.** (A) PAGE analysis of terminal crosslinking reaction resulting in a DNA hairpin. (B) UV thermal melting curves before and after crosslinking monitored at 260 nm. (C) Schematic representations of the nicked duplex for photoinduced ligation of  $T^{ol}dU$ . (D) Kinetics of ligation analyzed via PAGE (left y-axis) and fluorescence increase at 410 nm (right y-axis), with or without template. (1  $\mu$ M DNA in 10 mM sodium phosphate, 100 mM NaCl, pH 7.0)

The demonstrated versatility of the  $T^{ol}dU$  crosslinking reactions suggests many different applications in bionanotechnology, including the synthesis of DNA nanomaterials.<sup>7</sup> Here we explored if  $T^{ol}dU$  and the dC/ $T^{ol}dU$  ICL motif are compatible with a hybridization chain reaction (HCR). HCR is an isothermal assembly process of two DNA hairpins into a nicked double helix by a cascade of hybridization events that is triggered by an initiator strand.<sup>20</sup> To investigate  $T^{ol}dU$ -HCR, we designed two hairpin structures which contained two dC/ $T^{ol}dU$  mismatches in the stem region.<sup>21</sup> With the addition of an initiator strand a DNA duplex polymer will be formed, in which two  $T^{ol}dU$  units originally placed in the two different hairpins will form the  $T^{ol}dU$  dimer crosslink motif (Fig 4A). This will allow the crosslinking reaction to take place upon irradiation and an increase in fluorescence should be observed.

The setup was first designed and tested with unmodified DNA (Fig S16, S17), and then we incorporated  $T^{ol}dU$  into the hairpin strands (Fig S18). Analysis by agarose gel electrophoresis showed the successful formation of an approximately 2000 bp long product upon addition of 10 % of the initiator strand, while almost no duplex formation was observed for the hairpins alone in the absence of initiator. Upon irradiation of the HCR sample on a transilluminator light source, the covalent crosslinking reaction was initiated, and the supramolecular DNA polymer was transformed to a covalent polymer, that was further analysed by denaturing PAGE and visualized by staining with Sybr gold. We investigated various initiator concentrations and irradiation times and analysed HCR and crosslinking efficiency by denaturing PAGE. Covalently linked products with a size of more than 1000 bp were observed, indicating the effective cross-linking reaction of at least 40 dimeric dC/ $T^{ol}dU$  motifs have taken place after short irradiation of only two minutes (Fig 4B). Next, we examined the combined ability of covalent crosslink formation and fluorescence enhancement for the sensitive detection of DNA sequences by HCR. In order to use  $T^{ol}dU$ -HCR for DNA sequence detection, the fluorescence increase after addition of the initiator strand (i.e. the analyte) was measured under constant irradiation at 320 nm. The data in Fig 4C confirm the concentration-dependent response of the  $T^{ol}dU$ -HCR DNA sensing platform. At an initiator concentration of 5 nM, the fluorescence slowly increased to ca 180% within 15 min, while increasingly faster rates and higher final intensities were recorded at 10, 20 and 50 nM analyte concentration, reaching up to 400% within 5 min (Fig 4C). Importantly, no fluorescence increase was observed upon addition of a random DNA sequence that was not complementary to the toehold in H2 (negative control NC, red in Fig 4C). These results demonstrate a new variant of fluorescence-based DNA detection is solution, that has a shorter response time and works at lower hairpin probe concentrations than a previously reported HCR setup based on pyrene excimer formation.<sup>20c</sup>

In summary, we presented  $T^{ol}dU$  as new nucleobase analogue with distinct fluorescent properties depending on Watson-Crick base pairing status and arrangement in the DNA duplex. The hydrophobic stacking interactions of two properly positioned  $T^{ol}dU$  moieties enabled the photoinduced crosslinking reaction in three different arrangements at internal or terminal positions

of the hybridized DNA duplex. In addition, enhanced fluorescence emission was observed upon crosslink formation, suggesting that the new <sup>Tol</sup>dU dimer is rigidly embedded in the resulting DNA structure. Our analytical data are consistent with a photoinduced [2+2] cycloaddition of an alkyne of one <sup>Tol</sup>dU unit and the C5-C6 double bond of the other <sup>Tol</sup>dU nucleobase. As a proof-of-principle application we showed that <sup>Tol</sup>dU photocrosslinking is compatible with HCR and the fluorescence enhancement can be used for sensitive DNA sequence detection. Moreover, we anticipate that the universal nature of the new crosslink makes it a useful tool in biochemistry and beyond, for example as an alternative to enzymatic ligation or to build covalently linked DNA nanostructures.<sup>22</sup>

We thank Manuela Michel for contributions to the <sup>Tol</sup>dU phosphoramidite synthesis and acknowledge support by the University of Würzburg and the Deutsche Forschungsgemeinschaft (DFG).

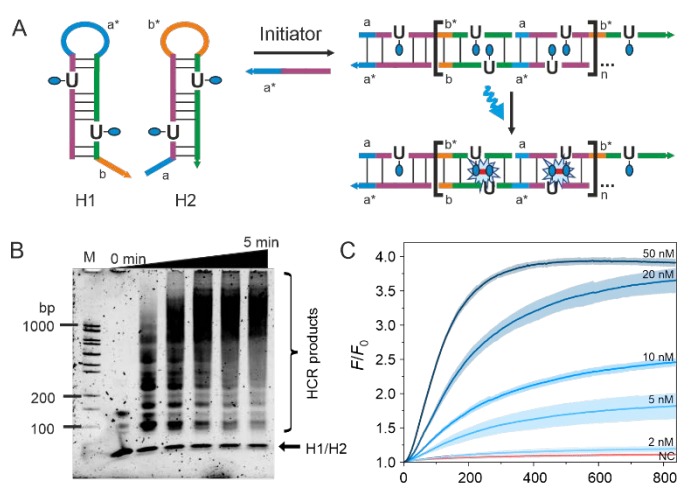


**Fig. 4.** (A) Illustration of the HCR with <sup>Tol</sup>dU containing hairpins H1 and H2. (B) Denaturing PAGE (5 %) of the irradiated HCR product at different timepoints (500 nM hairpins with 50 nM initiator in 75 mM sodium citrate, 750 mM NaCl, pH 7.0). (C) Fluorescence increase at 410 nm after addition of initiator DNA strand at 2, 5, 10, 20 or 50 nM concentration, NC is negative control strand at 50 nM (100 nM hairpins in 75 mM sodium citrate buffer, 750 mM NaCl, pH 7.0).

## Conflicts of interest

There are no conflicts to declare.

## Notes and references

1. a) W. Xu, K. M. Chan and E. T. Kool, *Nat Chem*, 2017, **9**, 1043-1055; b) D. Dziuba, P. Didier, S. Ciaco, A. Barth, C. A. M. Seidel and Y. Mely, *Chem Soc Rev*, 2021, **50**, 7062-7107.
2. B. Y. Michel, D. Dziuba, R. Benhida, A. P. Demchenko and A. Burger, *Front Chem*, 2020, **8**.
3. a) M. S. Wranne, A. F. Fuchtbauer, B. Dumat, M. Bood, A. H. El-Sagheer, T. Brown, H. Graden, M. Grotli and L. M. Wilhelmsson, *J Am Chem Soc*, 2017, **139**, 9271-9280; b) C. S. Eubanks, J. E. Forte, G. J. Kapral and A. E. Hargrove, *J Am Chem Soc*, 2017, **139**, 409-416; c) F. Wachowius and C. Höbartner, *Chembiochem*, 2010, **11**, 469-480.
4. a) A. Karimi, R. Borner, G. Mata and N. W. Luedtke, *J Am Chem Soc*, 2020, **142**, 14422-14426; b) A. Okamoto, K. Kanatani and I. Saito, *J Am Chem Soc*, 2004, **126**, 4820-4827.
5. a) Y. W. Jun, D. L. Wilson, A. M. Kietrys, E. R. Lotsof, S. G. Conlon, S. S. David and E. T. Kool, *Angew Chem Int Ed*, 2020, **59**, 7450-7455; b) P. Ghosh, H. M. Kropp, K. Betz, S. Ludmann, K. Diederichs, A. Marx and S. G. Srivatsan, *J Am Chem Soc*, 2022, **144**, 10556-10569.
6. Y. N. Teo and E. T. Kool, *Chem Rev*, 2012, **112**, 4221-4245.
7. M. Madsen and K. V. Gothelf, *Chem Rev*, 2019, **119**, 6384-6458.
8. K. Gorska and N. Winssinger, *Angew Chem Int Ed*, 2013, **52**, 6820-6843.
9. V. M. Lechner, M. Nappi, P. J. Deneny, S. Folliet, J. C. K. Chu and M. J. Gaunt, *Chem Rev*, 2022, **122**, 1752-1829.
10. a) K. Fujimoto, S. Matsuda, N. Takahashi and I. Saito, *J Am Chem Soc*, 2000, **122**, 5646-5647; b) T. Ihara, T. Fujii, M. Mukae, Y. Kitamura and A. Jyo, *J Am Chem Soc*, 2004, **126**, 8880-8881; c) L. Antusch, N. Gass and H. A. Wagenknecht, *Angew Chem Int Ed*, 2017, **56**, 1385-1389.
11. a) T. Gerling and H. Dietz, *Angew Chem Int Ed*, 2019, **58**, 2680-2684; b) K. Fujimoto, S. Sasago, J. Mihara and S. Nakamura, *Org Lett*, 2018, **20**, 2802-2805; c) H. Kashida, T. Doi, T. Sakakibara, T. Hayashi and H. Asanuma, *J Am Chem Soc*, 2013, **135**, 7960-7966; d) A. Manicardi, E. Cadoni and A. Madder, *Chem Sci*, 2020, **11**, 11729-11739.
12. a) D. K. Prusty and A. Herrmann, *J Am Chem Soc*, 2010, **132**, 12197-12199; b) K. Meguellati, G. Koripelly and S. Ladame, *Angew Chem Int Ed*, 2010, **49**, 2738-2742.
13. D. G. von Kruchten, M. Roth and O. Seitz, *J Am Chem Soc*, 2022, **144**, 10700-10704.
14. S. K. Albert, H. V. Thelu, M. Golla, N. Krishnan, S. Chaudhary and R. Varghese, *Angew Chem Int Ed*, 2014, **53**, 8352-8357.
15. L. H. Thoresen, G. S. Jiao, W. C. Haaland, M. L. Metzker and K. Burgess, *Chem Eur J*, 2003, **9**, 4603-4610.
16. H. Neitz, I. Bessi, V. Kachler, M. Michel and C. Höbartner, *Angew Chem Int Ed*, 2023, **62**, e202214456.
17. R. L. Letsinger, T. F. Wu, J. S. Yang and F. D. Lewis, *Photochem Photobiol Sci*, 2008, **7**, 854-859.
18. H. Neitz, I. Bessi, J. Kuper, C. Kisker and C. Höbartner, *J Am Chem Soc*, 2023, **145**, 9428-9433.
19. R. Carmieli, T. A. Zeidan, R. F. Kelley, Q. Mi, F. D. Lewis and M. R. Wasielewski, *J Phys Chem A*, 2009, **113**, 4691-4700.
20. a) R. M. Dirks and N. A. Pierce, *Proc Natl Acad Sci USA*, 2004, **101**, 15275-15278; b) S. Bi, S. Z. Yue and S. S. Zhang, *Chem Soc Rev*, 2017, **46**, 4281-4298; c) J. Huang, Y. R. Wu, Y. Chen, Z. Zhu, X. H. Yang, C. J. Yang, K. M. Wang and W. H. Tan, *Angew Chem Int Ed*, 2011, **50**, 401-404; d) A. L. Prinzen, D. Saliba, C. Hennecker, T. Trinh, A. Mittermaier and H. F. Sleiman, *Angew Chem Int Ed*, 2020, **59**, 12900-12908.
21. a) K. Morihira, Y. Moriyama, Y. Nemoto, H. Osumi and A. Okamoto, *J Am Chem Soc*, 2021, **143**, 14207-14217; b) C. A. Figg, P. H. Winegar, O. G. Hayes and C. A. Mirkin, *J Am Chem Soc*, 2020, **142**, 8596-8601.
22. a) K. Zhang and V. W. Yam, *Chem Sci*, 2020, **11**, 3241-3249; b) D. Wang, P. Liu and D. Luo, *Angew Chem Int Ed*, 2022, **61**, e202110666.